Recent Advances in Musculoskeletal MR Imaging

Initial Clinical Experience with an Iterative Denoising Algorithm Applied to Reduced-data 2D Turbo Spin Echo Acquisitions

Johan Dehem, M.D.; et al.
VZW Jan Yperman, Ypres, Belgium

Deep Resolve – Mobilizing the Power of Networks

Nicolas Behl, Ph.D.
Siemens Healthineers, Erlangen, Germany

Compressed Sensing in Metal Hip Imaging: Our Experience

Mustafa M. Almuqbel, RT, (MR), ARRT, Ph.D.; et al.
Pacific Radiology Group, Christchurch, New Zealand

Reprinted from **MAGNETOM Flash (77) 2/2020** and **MAGNETOM Flash (78) 1/2021**

SIEMENS Healthineers

Initial Clinical Experience with an Iterative Denoising Algorithm Applied to Reduced-data 2D Turbo Spin Echo Acquisitions

Johan Dehem, M.D.[1]; Stephan Kannengießer, Ph.D.[2]; Uvo Christoph Hoelscher, Ph.D.[2]

[1]Jan Yperman Ziekenhuis, Ieper, Belgium
[2]Siemens Healthineers, Erlangen, Germany

Introduction

Magnetic Resonance Imaging (MRI) with standard 2D Turbo Spin Echo (TSE) sequences is a trusted technique to guarantee excellent soft tissue contrast in musculoskeletal (MSK), neurological, and abdominal imaging. The signal and contrast behavior are well understood and appreciated by the reading radiologist and referring physicians alike. The acquisition time of these 2D TSE sequences is in the order of several minutes, hence has always been a point of attention. With the introduction of parallel imaging [1], acquisition times could be sped up, typically by an acceleration factor (p) of two or three, by only acquiring a fraction of the data lines in *k*-space and calculating the missing data lines taking into account the coil-sensitivity profiles. The well-known standard 2D TSE soft tissue contrast behavior is not affected by this acceleration. However, as a rule of thumb, higher acceleration factors do induce some noise in the image by a factor of $\sqrt{p}*G$ where G stands for geometry factor (G is close to 1 in a perfect system), limiting the practical acceleration factor to two or three. Note that it is common practice to combine parallel imaging and multiple averages, since motion effects can be minimized by the shorter acquisition times of the former, while regaining SNR with the latter, which has advantages over un-accelerated acquisitions of the same duration.

At the same time elaborate denoising methods have been developed which have to balance noise removal and preservation of details [2]. A recently introduced acceleration technique with strong data under-sampling, allowing for significantly higher acceleration factors, for example five or higher, is Compressed Sensing (CS) [3]. CS works best in combination with random undersampling of multi-dimensional data, and the reconstruction algorithm can achieve both image restoration and denoising. Pushed to the limit, the CS images may appear unnatural, so that both radiologist and referring physician need to get used to this new sequence, to gain experience with a new

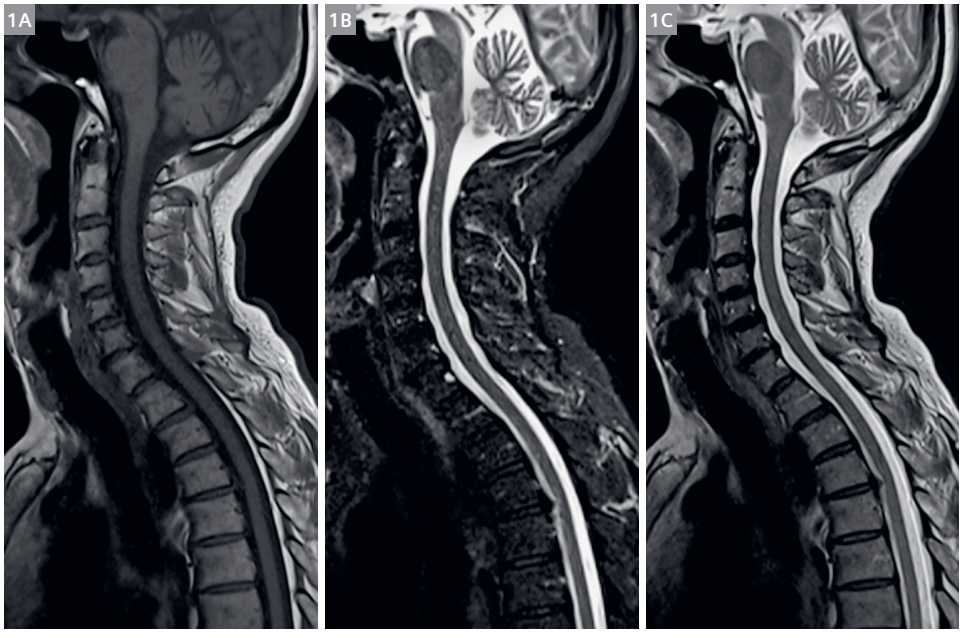

1 Parallel imaging p2: halving acquisition time with acceleration factor 2 comes with a signal loss by $\sqrt{2}*G$, best noticeable in the T2 stir images; acquisition time 46 seconds T1 TSE **(1A)**, 47 seconds T2 IR TSE **(1B)**, and 68 seconds T2 TSE **(1C)**.

signal and contrast behavior, a new look and feel of the soft tissue contrast. Regular 2D TSE data does not seem to be optimal for CS reconstruction.

Image reconstruction based on artificial intelligence (AI) / deep learning (DL) is the latest development capable of denoising [4]. These techniques, however, require large amounts of training data, which was beyond the scope of this study.

Iterative denoising (ID) is a technique which uses similar noise-suppressing operations as Compressed Sensing, but which is specifically designed to be combined with standard parallel imaging and other standard imaging techniques, allowing for shorter scan times and/or higher resolution while compensating for the resultant SNR loss [5]. First applications focused on volumetric acquisitions [6]. This study presents initial experience with this technique applied to standard 2D TSE data in multiple body regions.

Methods and materials

The goal of this study was to investigate whether the new iterative denoising technique can compensate for the resultant SNR loss when using higher acceleration in standard 2D TSE imaging. To make this comparison between images with higher acceleration versus standard acceleration as accurate as possible, instead of rescanning patient with higher acceleration factors, higher acceleration was simulated by discarding one average from the raw data sets. By applying this simulated acceleration, it was possible to obtain datasets that are – except for the virtual acceleration – completely identical.

Eleven clinical data sets from the perineum, uterus, prostate, l-spine, and sacroiliac joint were acquired on a 1.5T clinical MR scanner (MAGNETOM Sola, Siemens Healthcare, Erlangen, Germany) with the standard turbo spin echo (TSE) sequence. Raw data allowing retrospective image reconstruction with subsets of the originally acquired averages was collected from regular patient examinations so that no additional or modified scans had to be performed. Informed consent from patients was obtained to reprocess anonymized data for clinical research. All raw data sets featured Parallel Imaging under-sampling and comprised two or more signal averages.

Data processing was performed offline and with the help of a prototype implementation of the ID algorithm as described in [4], integrated into the image reconstruction pipeline. Quantitative noise measurements were drawn from the system's adjustment framework. Taking into account all noise-modifying operations, a noise map was calculated which describes the spatial noise distribution in coil-combined, complex-valued images after the parallel imaging reconstruction [7, 8]. Then the wavelet thresholding is automatically adjusted for MMSE-optimal noise removal according to "Stein's Unbiased Risk Estimator" (SURE) [9]. This automated parameter selection allows the algorithm to adapt to both the noise and signal characteristics of each individual image and to generalize to multiple body regions and scan protocols without additional manual tuning. Some edge enhancement was applied after the ID to compensate for perceived loss in sharpness.

From each multi-average raw data set three different versions of the images were reconstructed. The first version (called "original") used all available averages and corresponds to the regular reconstruction; it does not use the denoising algorithm. To simulate accelerated acquisition, the second reconstruction version discarded one signal average from the raw data sets, e.g. one out of two; it also did not use the iterative denoising algorithm and is called "accelerated". The third reconstruction version discarded the same signal average from the raw data sets, and additionally applied the described iterative denoising algorithm. These images are called "accelerated + ID".

The versions "accelerated" and "accelerated + ID" simulate accelerated acquisition by lowering the number of averages. With this simulation approach the three versions are based upon as similar data sets as possible so that they can be directly compared. They derive from the same acquisition so that all variations between repeated scans can be avoided. However, the data is not identical because version two and three only use a subset of the data. Hence effects like physiological motion still can have a different effect on the different versions – especially if the motion happens during the discarded part of the raw data.

The described versions of the images were viewed side-by-side on an open source DICOM viewer (Horos™) and ranked by an experienced radiologist according to image quality in terms of perceived signal to noise ratio as well as noticeable artifacts like blurring. Any non-diagnostic image quality was marked. Given the obvious differences between the image versions, no effort at blinding was made.

Results

Table 1 lists the ranking results. In 10 out of 11 cases (91%), the "original" version was ranked best. Of the "accelerated" versions, study 2 (Figs. 2, 3) is no longer diagnostic (marked as X). All "accelerated + ID" versions were ranked better than the "accelerated" versions, and all were diagnostic. In study 5 (Fig. 5) the image quality in the "accelerated + ID" version equals the image quality of the "original" version. In study 11 (Figs. 7, 8) the image quality of the "original" is less than the image quality of both the "accelerated + ID" images and "accelerated" images. Example image features are described in the figure captions.

study #	contrast	# of averages, [timesaving]	best image	2nd best image	3rd best image
1	STIR SI joint, cor	2 [50%]	"original"	"accelerated + ID"	"accelerated"
2	STIR L-spine, sag	2 [50%]	"original"	"accelerated + ID"	"accelerated" (X)
3	T1 L-spine, sag	2 [50%]	"original"	"accelerated + ID"	"accelerated"
4	T1 L-spine, sag	2 [50%]	"original"	"accelerated + ID"	"accelerated"
5	T2 uterus, cor	3 [33%]	"original" = "accelerated + ID"	"accelerated"	–
6	T2 prostate, ax	3 [33%]	"original"	"accelerated + ID"	"accelerated"
7	STIR SI joint, cor	2 [50%]	"original"	"accelerated + ID"	"accelerated"
8	STIR SI joint, cor	2 [50%]	"original"	"accelerated + ID"	"accelerated"
9	STIR SI joint, cor	2 [50%]	"original"	"accelerated + ID"	"accelerated"
10	T2 uterus, sag	2 [50%]	"original"	"accelerated + ID"	"accelerated"
11	T2 perineum, ax	4 [25%]	"accelerated + ID"	"accelerated"	"original"

Table 1: Results from the side-by-side reading of an experienced radiologist.

Study 2

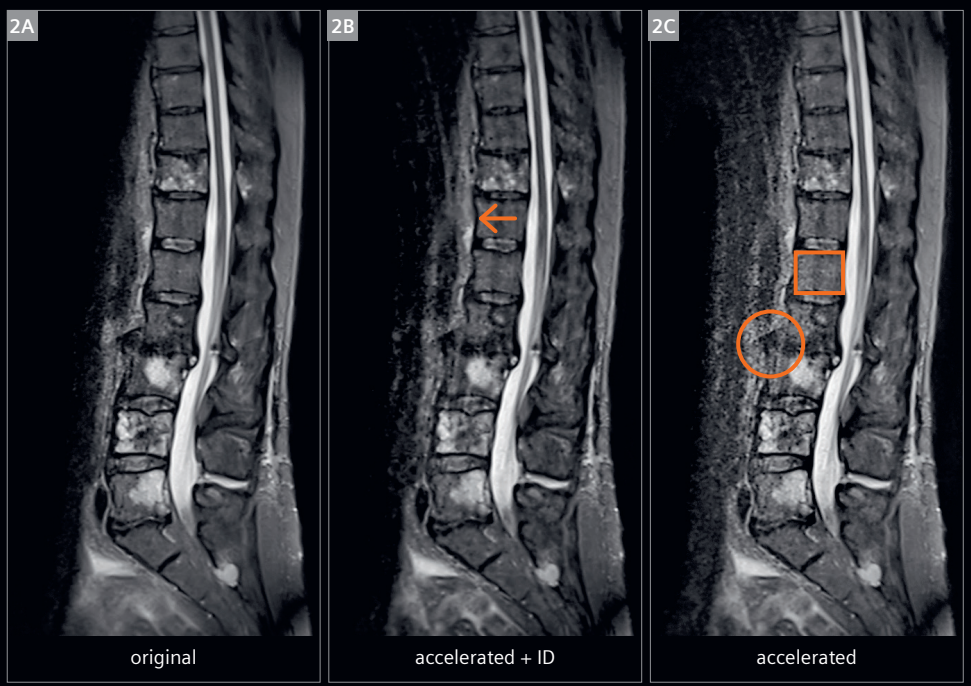

2 The "original" version **(2A)** with two averages has the best image quality since two averages are effectively averaging out the ghosting artifact. On top of the ghosting, version "accelerated" **(2C)** has a very low SNR with a "grainy unsharpness" e.g. in the body of vertebra L1 (square box) or prevertebral space (red circle) and intervertebral space level L2–L3 making this image non-diagnostic. In version "accelerated + ID" **(2B)** the "grainy blurriness" is effectively removed (arrow points to substantial SNR gain in prevertebral space). This leads to a still challenging but more diagnostic image quality resembling the morphology and contrast of the "original" version, e.g. in the endplates L2–L3. Simulated acquisition time saving: 50%. Scanning parameters: TE 99 ms, TR 4570 ms, TI 140 ms, duration for original (two averages) 1:17 min.

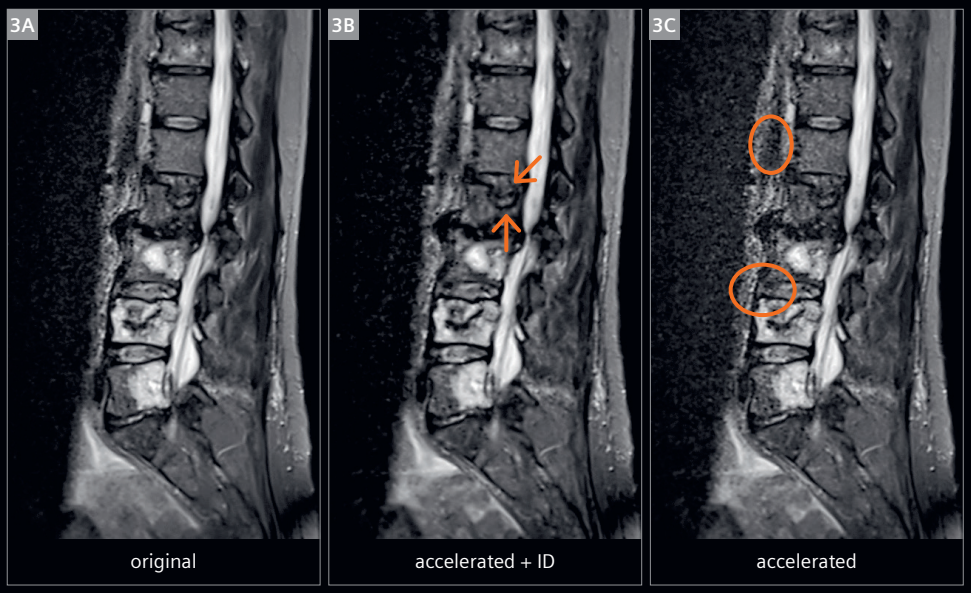

3 Same patient as Figure 1. Image zoomed in and slightly off midline. Version "accelerated" **(3C)** is severely impaired by both low SNR and ghosting artifact. The exaggerated noise level makes it of questionable diagnostic value (red circles indicate low SNR).Version "accelerated + ID" **(3B)** still suffers from ghosting artifact, however the ID algorithm processing of the image effectively removes the grainy pattern over the vertebral bodies and prevertebral fat plane. The resulting image quality improvement makes it easy to delineate the intravertebral disc herniation (red arrows).

Study 3

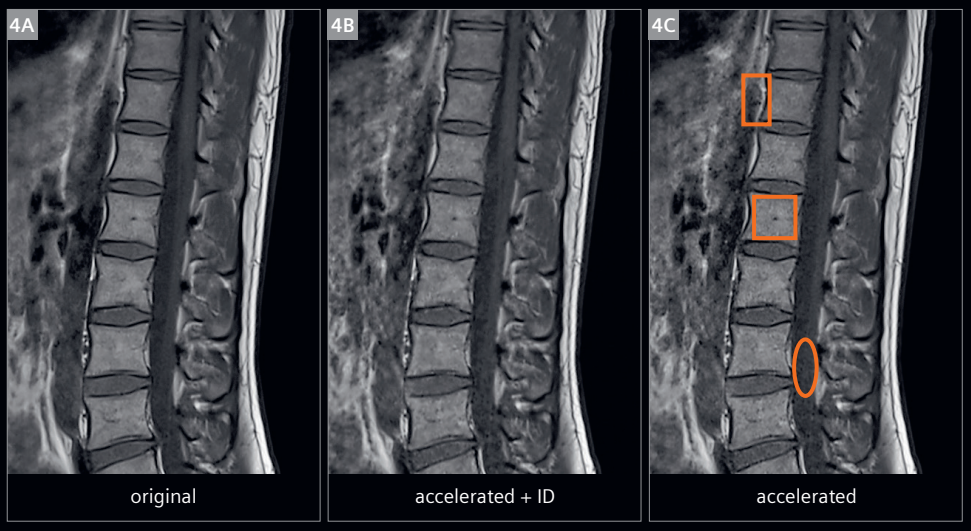

4 The "original" version **(4A)** with two averages has crisp image quality in this "perfect patient". Version "accelerated" **(4C)** features an exaggerated noise level in comparison to the "original" (red squares). The SNR of version "accelerated + ID" **(4B)** is still lower than in the "original" version; however, in comparison to the "accelerated" version SNR is clearly higher. Simulated acquisition time saving: 50%. Scanning parameters: TE 8 ms, TR 603 ms, duration for original 1:38 min.

Study 5

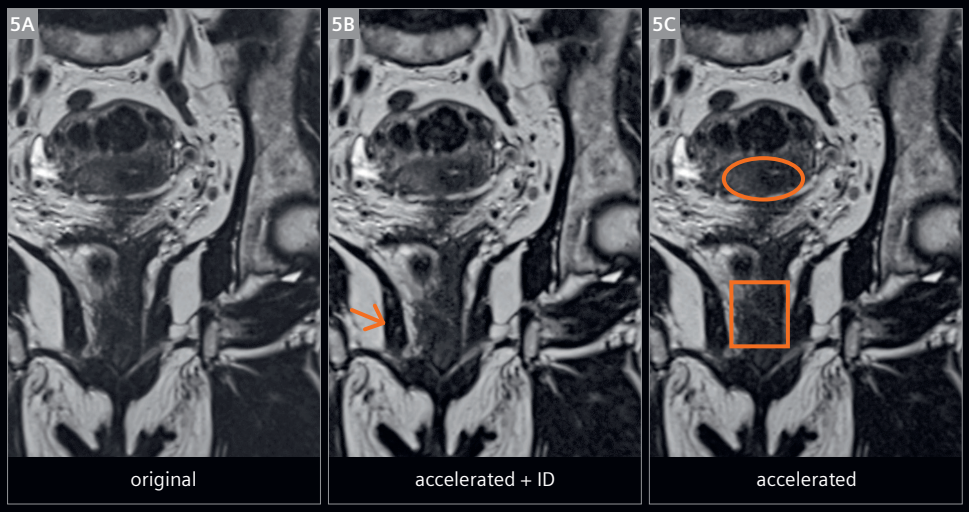

5 All three images are of diagnostic quality with high signal. Some graininess indicating lower SNR is present in the "accelerated" image **(5C)** over the uterus (red oval) and vagina (red box). This grainy superposition is removed after ID in version "accelerated + ID" **(5B)**. The resulting image in version "accelerated + ID" (center) matches very closely the image quality of the "original" version **(5A)**. The version "accelerated + ID" (center) has the highest overall SNR without graininess. Taking a closer look at details e.g. the fatty streaks in the right ischiococcygeal muscle (red arrow): these small fatty streaks are depicted with the same confidence as on the original image, indicating that no image detail is lost during ID. Simulated time saving: 33%. Scanning parameters: TE 132 ms, TR 7780 ms, duration for original 1:25 min.

Study 7

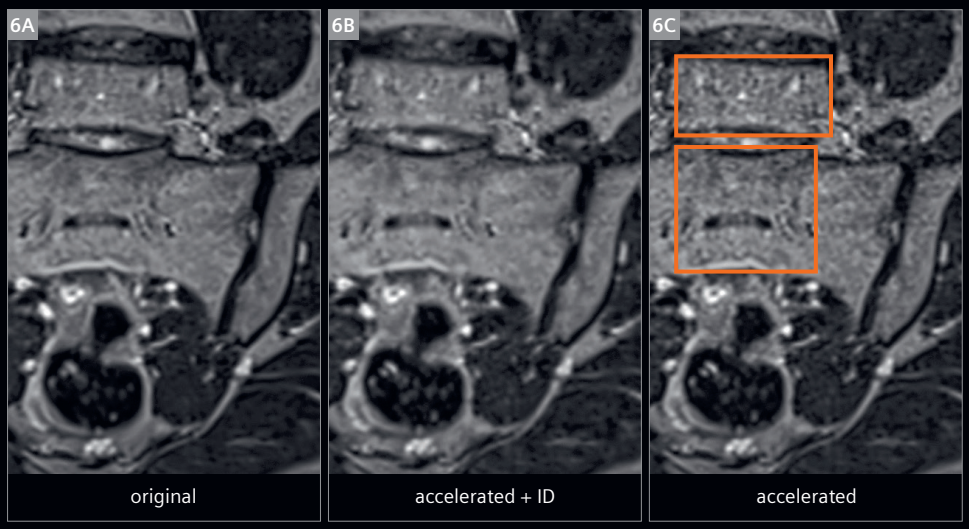

6 The "original" version **(6A)** with two averages has the best image quality. Version "accelerated" **(6C)** has a low signal to noise with impressive "graininess" (square boxes) over the fifth lumbar and first sacral vertebra. In version "accelerated + ID" **(6B)** the overlying "graininess" is effectively removed resulting in an image with SNR resembling the "original" version. Simulated acquisition time saving: 50%. Scanning parameters: TE 87 ms, TR 3400 ms, TI 140 ms, duration for original 0:52 min.

Study 11

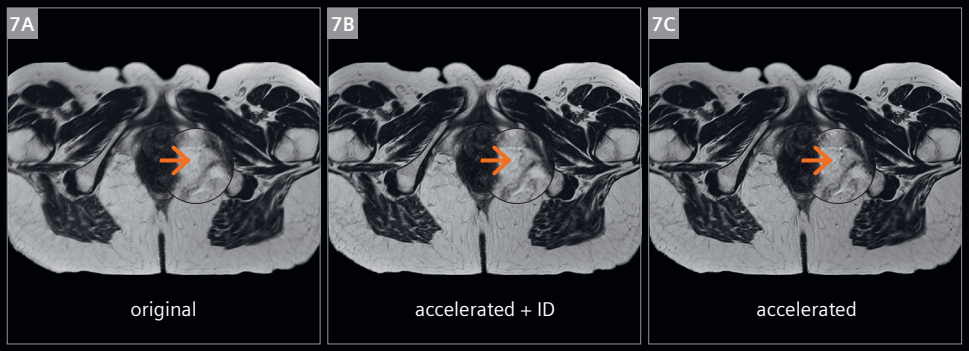

7 Version "original" **(7A)** has abundant signal, however, some blurring is present. Version "accelerated" (right) and "accelerated + ID" **(7B)** have less blurring since less measurement time leads to less patient movement, but still have abundant signal. This abundance in signal results in an image quality where for instance the veins in the ischiorectal fossa are better depicted in both versions "accelerated" **(7C)** and "accelerated + ID" (center) than on the original version. Although high enough SNR is present in version "accelerated" (right), ID further enhances the image quality in "accelerated + ID" (center) image: the small venous bifurcation (red arrow, magnifying glass) in the left ischiorectal fossa is better depicted after ID (center). Simulated time saving: 25%. Scanning parameters: TE 106 ms, TR 814 ms, duration for original 4:12 min.

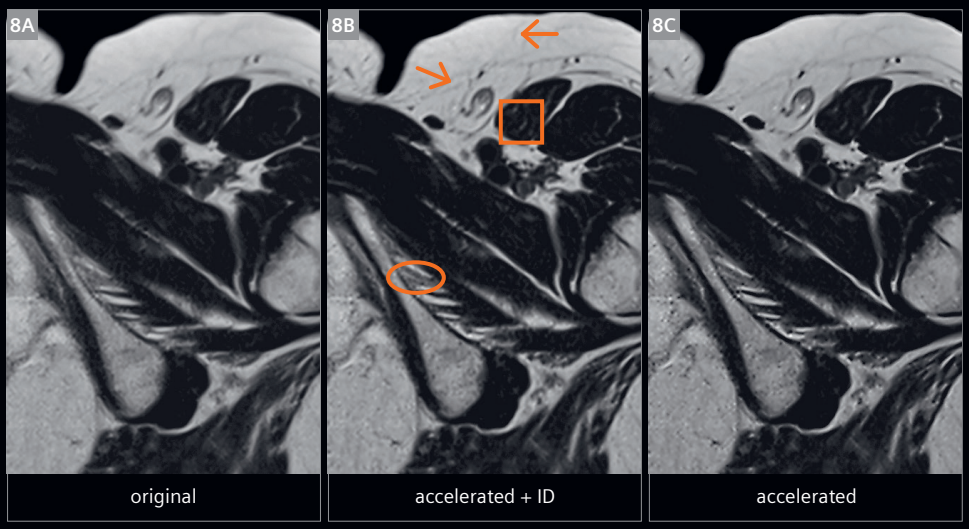

8 Same study as Figure 7: In version "original" **(8A)** the small fibrous strands in subcutaneous fat are hard to depict even though they are clearly present on the "accelerated" version **(8C)** and really stand out on the "accelerated + ID" version (red arrows). The fatty streaks (red circle) in between the muscle fibers of the external obturator cannot be seen on the "original" version, they are however visible on the "accelerated" version and really stand out on the "accelerated + ID" version **(8B)**. The ID algorithm does not only increase SNR but also enhances image details, for example the fatty streaks in the iliac muscle (red box). The internal structure with fat-containing hilum of the left inguinal lymph node (between the red arrow and red box) is again best depicted on the "accelerated + ID" version. Simulated time saving: 25%. Scanning parameters: TE 106 ms, TR 814 ms, duration for original 4:12 min.

Discussion

Acquiring a dataset that is substantially accelerated (by reducing the number of averages) leads to a discernible drop in signal to noise ratio. This is rendering the resulting images grainy and harder or even sometimes impossible to interpret, with an obvious drop in image quality in comparison to the "original" images. The results of this small-scale study provide evidence that the process of ID as described above can compensate for the drop in signal to noise ratio in substantially accelerated 2D datasets.

In this study the perceived gain in image quality after ID was obvious in images which are already by design inherently lower in signal to noise ratio like e.g. Short-TI Inversion Recovery (STIR) imaging. Studies 7 and 8 with coronal STIR imaging of sacroiliac joints demonstrate the benefit from the ID bringing image quality back to the standard imaging quality. Apparently, ID is reducing the noise level in the signal and image quality thereby approaches the image quality of the "original" images.

Less intuitive, even in images with abundant signal, the image quality of "accelerated + ID" can be as good (study 5) or even better (study 11) than the original. A plausible explanation is that by removing an average also removes the blurring that can occur due to slight patient movement between multiples averages.

Iterative denoising, in contrast to conventional noise-removing image filters, has the advantage of supplementary quantitative noise distribution information, which would otherwise have to be estimated from the images themselves. Consequently, over- or under-filtering is inherently avoided. In combination with the SURE-optimizing iteration, this is especially important for preserving small image details and sharpness, although some additional edge enhancement appears to be beneficial. Preserved image details and sharp edges are striking in study 11 (Figs. 7) where the small venous bifurcation in the left ischiorectal fossa is clearly sharper delineated in the "accelerated + ID" image than on the images without denoising. Figure 8 is another excellent example that no over-filtering occurs: the small septae in the subcutaneous fat are better depicted on the accelerated images with denoising when compared to the accelerated version as well as to the original version. This can be seen in the fatty streaks in the external obturator muscle.

Conclusion

Image quality in standard 2D MRI sequences, accelerated in simulation beyond the threshold of standard acceptable noise levels, can be substantially improved by applying an ID algorithm using supplementary information about the image noise level. It is expected that standard 2D MRI can profit from ID when natively scanning with lower numbers of averages and hence shorter acquisition times. More clinical studies with different clinical perspectives are required to show if ID could become as indispensable a tool in MRI as iterative reconstruction is in CT.

Contact

Johan Dehem, M.D.
Jan Yperman Ziekenhuis
Briekestraat 12
8900 Ypres
Belgium
Phone: +32 57 35 74 00
johan.dehem@yperman.net

Acknowledgements

The authors are grateful to Dr. Boris Mailhe for developing the core of the iterative denoising technique and Dr. Carmel Hayes for her support in algorithm implementation and data processing.

References

1 Heidemann RM et al. A brief review of parallel magnetic resonance imaging. European Radiology, Vol 13 2003: 2323–2337.
2 Mohan J, Krishnavenib V,and Guo Y. A survey on the magnetic resonance image denoising methods. Biomed Signal Process Control, Vol 9 2014: 56-69.
3 Geethanath S et al. Compressed sensing MRI: a review. Crit Rev Biomed Eng, Vol 41(1) 2013: 183-204.
4 Lin DJ et al. Artificial Intelligence for MR Image Reconstruction: An Overview for Clinicians. J Magn Reson Imaging 2020 Feb 12. Online ahead of print.
5 Kannengiesser SAR et al. Universal iterative denoising of complex-valued volumetric MR image data using supplementary information. Proc. Intl. Soc. Mag. Reson. Med., Vol 24 2016: 1779.
6 Kang HJ et al. Clinical Feasibility of Gadoxetic Acid-Enhanced Isotropic High-Resolution 3-Dimensional Magnetic Resonance Cholangiography Using an Iterative Denoising Algorithm for Evaluation of the Biliary Anatomy of Living Liver Donors. Invest Radiol., Vol 54(2) 2019: 103-109.
7 Breuer FA et al. General formulation for quantitative G-factor calculation in GRAPPA reconstructions. Magn Reson Med., Vol 62(3) 2009: 739-46.
8 Kellman P, and McVeigh ER. Image reconstruction in SNR units: a general method for SNR measurement. Magn Reson Med., Vol 54(6) 2005: 1439-47.
9 Blu F, and Lusier T. The SURE-LET Approach to Image Denoising. IEEE Trans Im Proc, Vol 16:11 2007: 2778 - 2786.

Deep Resolve – Mobilizing the Power of Networks

Nicolas Behl, Ph.D.

Global Marketing Manager MRI Systems, Siemens Healthineers, Erlangen, Germany

The limitations of conventional image reconstruction

MRI is established as one of the key modalities in diagnostic imaging. The absence of ionizing radiation and the unmatched soft tissue contrast distinguish MRI from other imaging modalities. While these features have helped to establish MRI as the method of choice for the diagnosis of many pathologies, the main limitation of MRI is the acquisition time.

With conventional reconstruction methods, the acceleration of an acquisition can only be achieved by accepting compromises with respect to image resolution or signal-to-noise ratio (SNR). In general, acquisition speed, image resolution, and SNR are tightly linked and increasing one of the three automatically has a negative effect on at least one of the two others (Fig. 1).

The use of receive arrays and parallel imaging has been an important breakthrough in MR image reconstruction and is an essential part of clinical routine in MRI [1, 2].

Parallel imaging, however, usually comes at the price of higher image noise, especially in regions further away from the receive coils. This results in inhomogeneous noise distribution, especially if high acceleration factors are used. Compressed Sensing was another major development when it comes to image acceleration [3]. It benefits especially dynamic and non-cartesian 3D imaging but comes at the cost of a higher computational burden. Also, 2D cartesian imaging, which still is building the backbone of routine MR imaging, benefits less from Compressed Sensing.

Over the last years, artificial intelligence (AI) technologies have made their appearance in a various research publications [4, 5]. Especially the use of deep neural networks has proven to be helpful when trying to address the limitations of conventional MR image reconstruction, especially also for routine 2D imaging. Deep learning image reconstruction has the potential to tackle all three limiting factors of MR imaging simultaneously: image resolution, SNR, and acquisition speed.

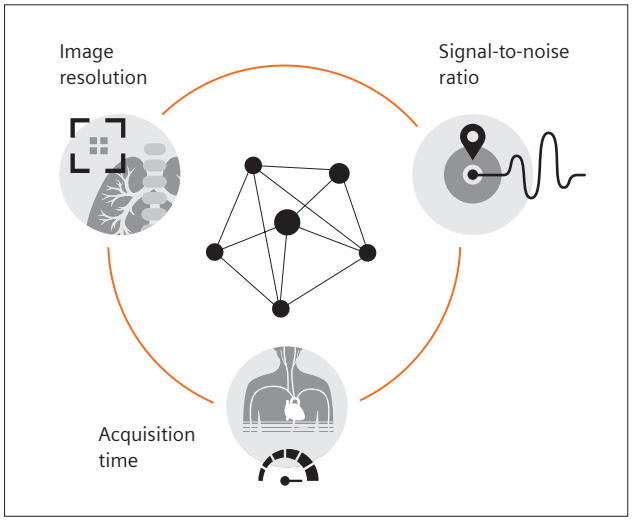

1 Image resolution, SNR, and acquisition time are the three limiting factors of MRI. Using conventional methods, changing one of them directly affects at least one of the two others. Deep learning reconstruction has the potential to disrupt this convention.

Deep Resolve Gain & Deep Resolve Sharp

Deep Resolve brings deep learning and AI to the MR image reconstruction process. Deep Resolve is an advanced reconstruction technology, which in its first step brings intelligent denoising and deep-learning-based image reconstruction directly to the core of the imaging chain.

Deep Resolve Gain is a solution for intelligent denoising. As mentioned above, in MRI, image noise is not uniformly distributed across the image. This can be due to coil array geometries since the SNR is usually higher close to the receive coils. Also the use of parallel imaging reconstruction techniques can lead to varying noise levels in the reconstructed image. These local variations in image noise can not be addressed by conventional noise filters, as these operate globally on the entire reconstructed image. Deep Resolve Gain incorporates specific noise maps, which are acquired together with the original raw data, directly into the image reconstruction [6].

These noise maps are generated without needing to spend additional scan time and can be extracted from the raw data. The reconstruction algorithm takes local noise variations into account and enables stronger denoising where noise would be most dominant when reconstructing with conventional methods.

Deep Resolve Gain helps to mitigate noise that is introduced when accelerating the acquisition e.g. by reducing

the number of averages or by increasing the acceleration factor in parallel imaging.

As the noise maps can be generated from the originally acquired raw data, no additional acquisition time is needed, and the results are available in real-time. Figure 2 shows how Deep Resolve Gain can be employed to accelerate an entire knee exam. Images acquired with increased acceleration and reconstructed with Deep

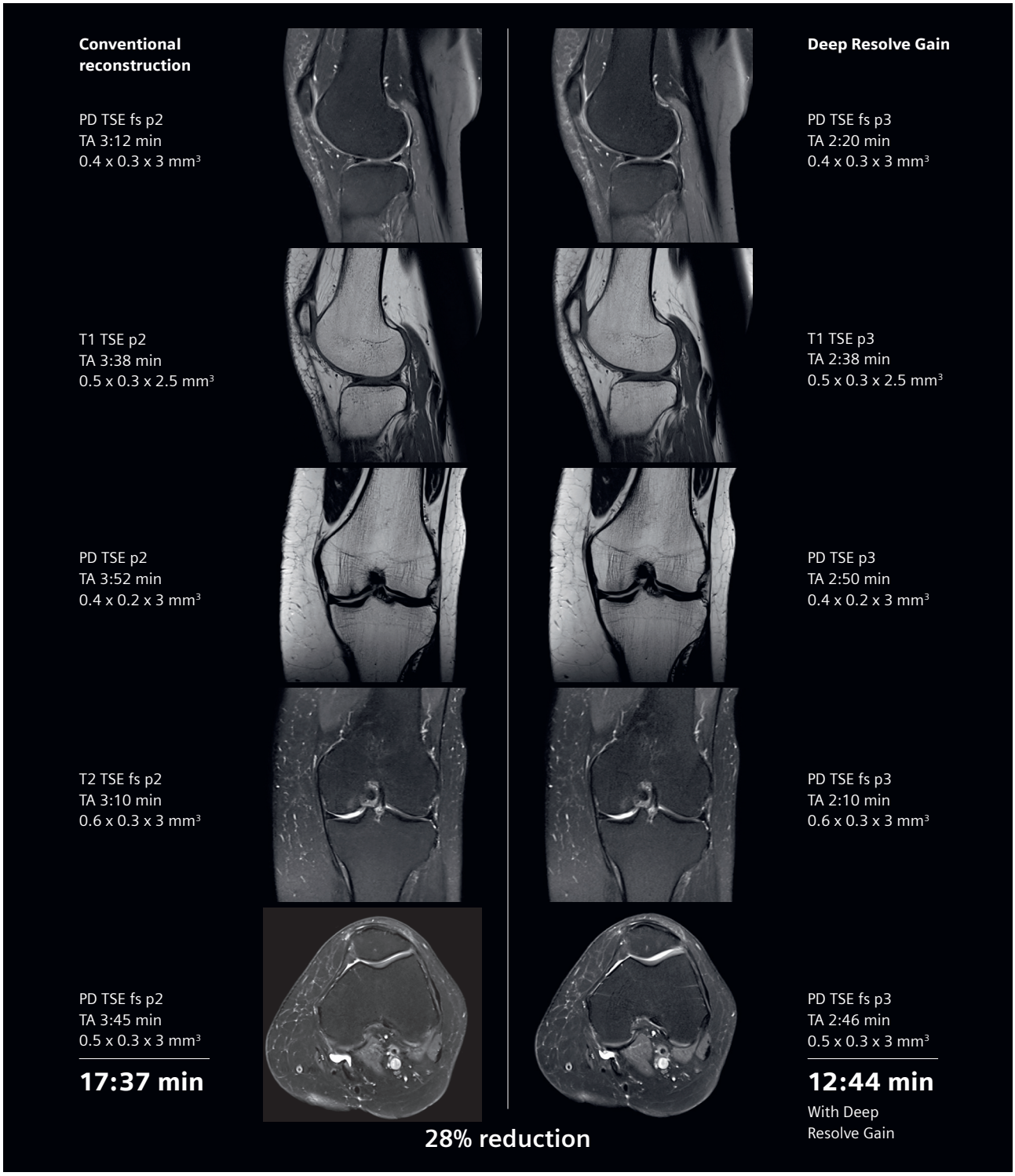

2 The increase in SNR achievable with Deep Resolve enables you to accelerate entire knee exams. The targeted reduction of image noise allows for the use of higher acceleration factors, without having to pay with increased image noise. Images are acquired on a MAGNETOM Vida 3T scanner.

Resolve Gain are similar in quality to the standard protocols which are conventionally reconstructed. In this example it results in an acceleration by 28% over the entire exam.

Deep Resolve Sharp is a novel image reconstruction technology to generate images with increased sharpness. The deep neural network at the core of Deep Resolve Sharp generates a high-resolution image from low resolution input data. The network was trained on a large number of pairs of low-resolution and high-resolution data.

As the training data for Deep Resolve Sharp covered a wide range of anatomies, the reconstruction network can be applied to all body regions. Deep Resolve Sharp can increase the matrix size by a factor of up to two along both in-plane axis, resulting in substantially increased image sharpness.

To ensure robust results, the acquired raw data is directly incorporated into the reconstruction and ensures consistency with the data from the scanner. The inclusion of the cross-check with the acquired raw data is essential for the robustness of the reconstruction and to ensure that contrasts are correctly represented in the final output. Figure 3 shows how Deep Resolve Sharp can be used to increase the sharpness of reconstructed images, without having to extend the acquisition time. Deep Resolve Sharp

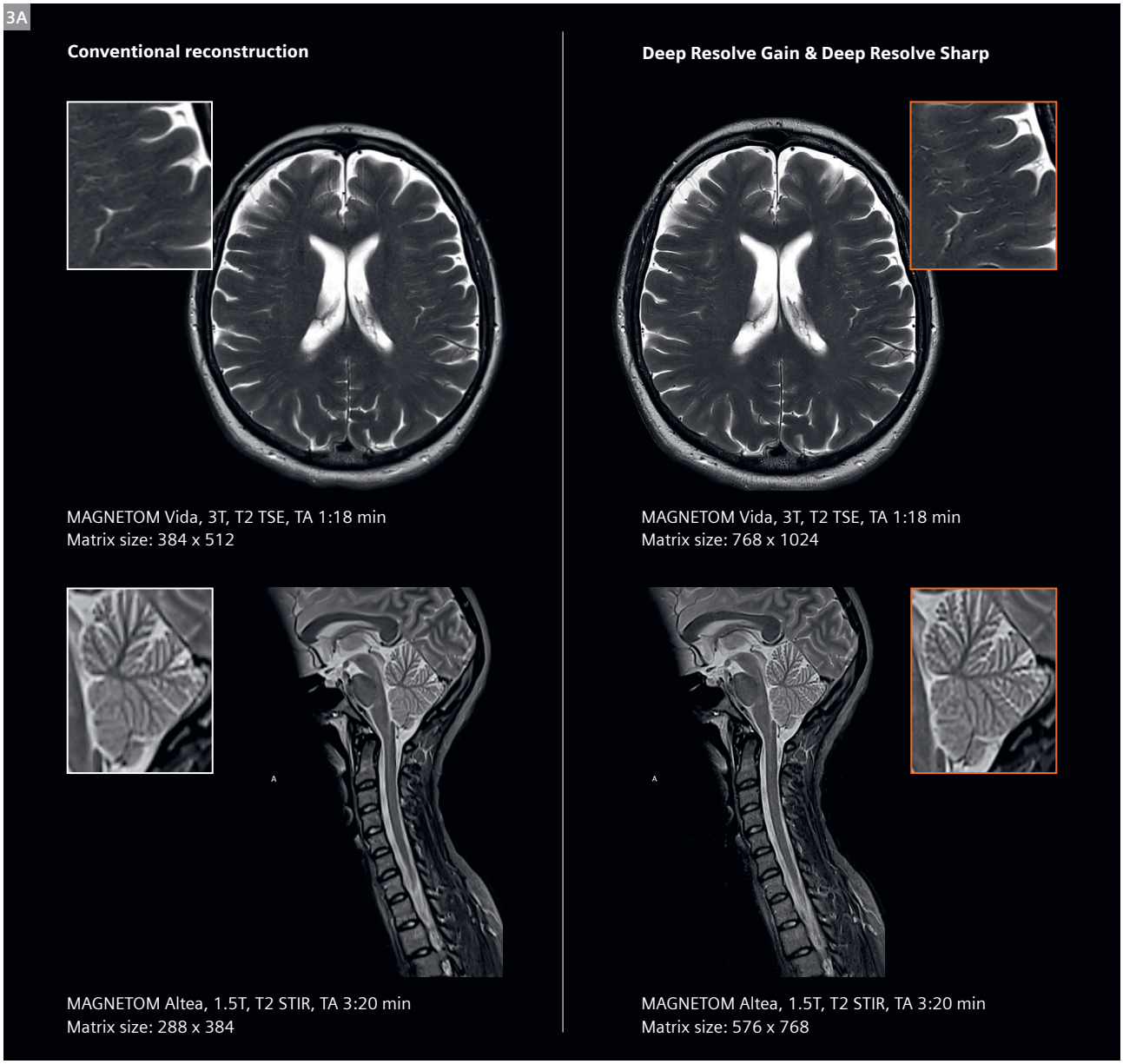

3 Deep Resolve Sharp uses a deep neural network to generate sharper images than ever before, enabling a clear depiction of fine structures and sharp edges. The use of raw data within the reconstruction process ensures robust results.

3B

Conventional reconstruction

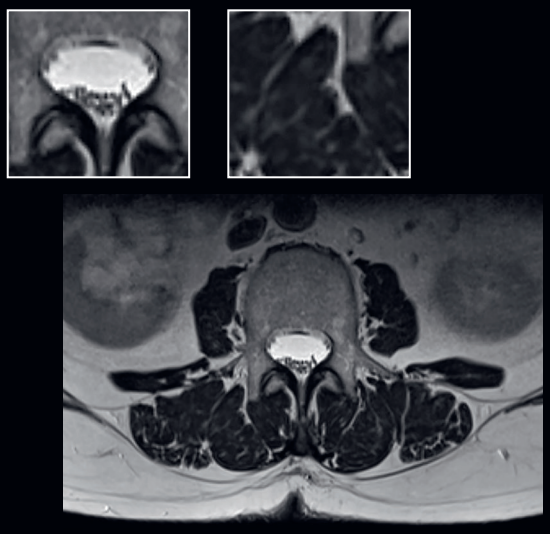

MAGNETOM Sola, 1.5T, T2 TSE, TA 3:45 min
Matrix size: 256 x 320

MAGNETOM Sola, 1.5T, T2 TSE, TA 2:24 min
Matrix size 307 x 384

Deep Resolve Gain & Deep Resolve Sharp

MAGNETOM Sola, 1.5T, T2 TSE, TA 3:45 min
Matrix size: 512 x 640

MAGNETOM Sola, 1.5T, T2 TSE, TA 2:24 min
Matrix size 614 x 768

1aaaa3595

1aaaa3588

can also be used to enable quicker scans. The phase resolution can be reduced in the acquisition and Deep Resolve Sharp can be employed to recover the resolution in the reconstruction process. An example is given in Figure 4B.

In Figure 4 you can see how Deep Resolve enables accelerated acquisition while simultaneously increasing image quality and sharpness.

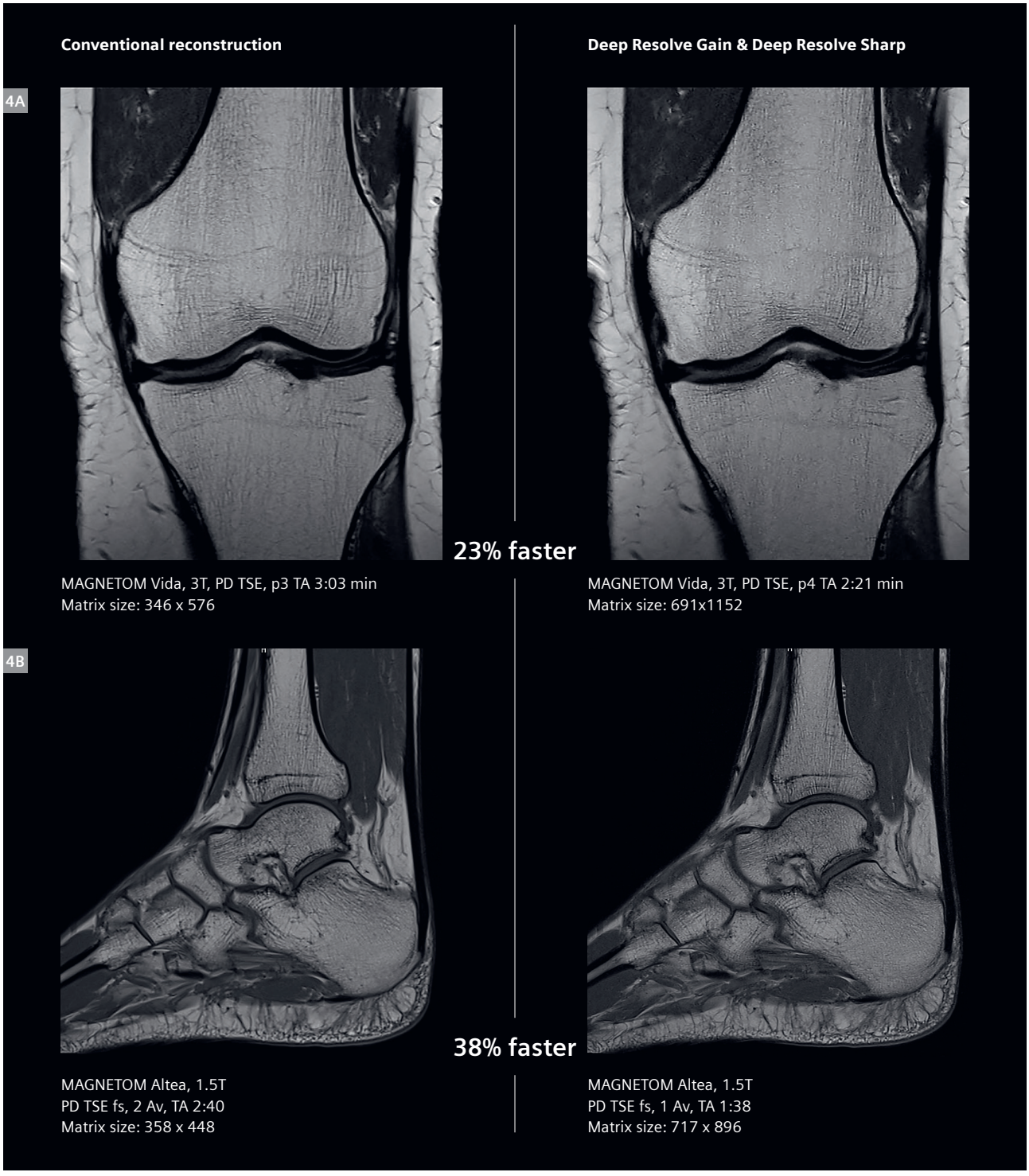

4 Together, the Deep Resolve technologies enable faster acquisitions, while increasing the image sharpness simultaneously. The targeted denoising achieved with Deep Resolve Gain allows for the use of higher acceleration, while Deep Resolve Sharp increases the sharpness of the image by increasing the matrix size.

Technology corner

Deep Resolve Gain uses individual noise maps as input for an iterative reconstruction process. This iterative process, together with the noise maps as prior knowledge reflecting where more noise is to be expected in the image, enables an effective denoising in the reconstruction process. This is similar to the reconstruction process used in Compressed Sensing, extending it to cartesian 2D imaging. For Deep Resolve Gain, the denoising in every iteration step takes place in the wavelet-domain. Denoising in the wavelet domain is more efficient than denoising in image or frequency domain. It enables a better separation between noise and small structures that are part of the image to be reconstructed. The denoising strength of Deep Resolve Gain can be adjusted, depending on the amount of noise and personal preference.

Deep Resolve Sharp uses a deep neural network to increase the sharpness in reconstructed images. The convolutional neural network operates on complex data and enables a reduction of the voxel size by up to a factor of two along each axis in-plane compared to conventional reconstruction. During the reconstruction using Deep Resolve Sharp, the information content corresponding to the originally acquired raw data remains unaffected. Incorporating the acquired raw data along the reconstruction process ensures robust results and correct representation of image contrast. The deep neural network used in Deep Resolve Sharp is rather used to predict the contents of remote areas within *k*-space. Conventional reconstruction using interpolation expands *k*-space with zeros, therefore not adding any information or contributing to image sharpness. The neural network at the core of Deep Resolve Sharp, on the other hand, was trained with a large number of pairs of low- and high-resolution data. It can therefore enhance the image with meaningful information corresponding to the outer parts of *k*-space, beyond the originally acquired data.

Open innovation platform[1]

Deep learning reconstruction is a very active field for researchers, demonstrating great potential for the future of MR image reconstruction, including denoising, artifact reduction, and possibly even the reconstruction of multiple contrasts from one single acquisition [7]. Deep Resolve gives you access to the plentitude of deep learning applications being developed in the field. Via an open innovation interface, Deep Resolve is planned to enable our partners to position their solutions in the Digital Marketplace, powered by the teamplay Digital Health Platform.

Currently, prototyping for image reconstruction algorithms is usually done offline, which means that the raw data has to be transferred from the scanner to a workstation, where they are finally reconstructed using a prototype developed e.g. in MATLAB or Python. These reconstructions then have to be converted to DICOM again if a clinician wants to evaluate them for a clinical study. Deep Resolve is planned to facilitate clinical transition for image reconstruction prototypes by enabling online reconstruction, directly at the scanner. The open innovation protocol is designed to support open community standards, such as the ISMRM raw data format and Gadgetron (Fig. 5).

[1] *The product is still under development and not commercially available yet. Its future availability cannot be ensured.*

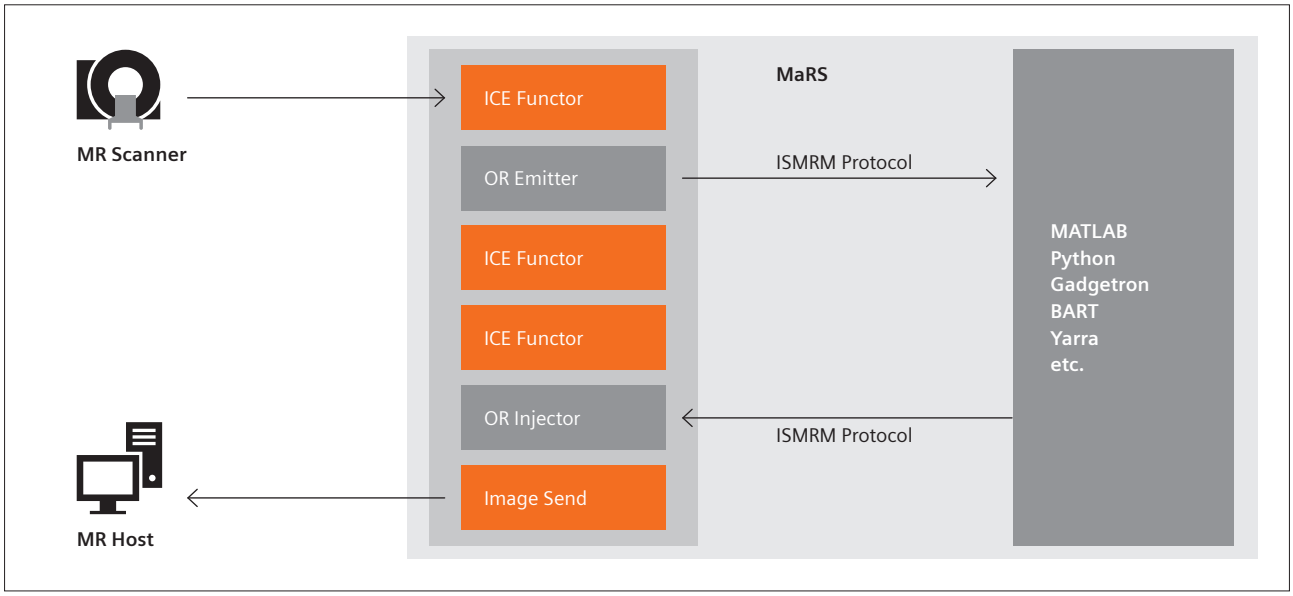

5 With an open innovation protocol, Deep Resolve is planned to facilitate translational research by enabling researchers to run their image reconstruction prototypes directly on the scanner.

Conclusion

Deep Resolve Gain and Deep Resolve Sharp introduce targeted, iterative denoising and deep learning reconstruction into clinical imaging. These technologies enable us to reduce acquisition times and improve image quality simultaneously. The unique inclusion of individual noise maps in an iterative reconstruction process enables intelligent, targeted denoising and Deep Resolve Sharp leverages the potential of deep learning reconstruction to achieve image resolutions beyond what is possible with conventional reconstruction methods. All this is done while including the acquired raw data along the entire reconstruction process, therefore ensuring robust and consistent results.

The potential of deep learning image reconstruction is immense, and current research is indicating a multitude of fascinating applications to come. Collaboration is key in MRI, so let us join our efforts in driving this exciting technology forward!

References

1 Pruessmann KP, Weiger M, Scheidegger MB, et al. SENSE: sensitivity encoding for fast MRI. Magn Reson Med. 1999;42(5):952-962.
2 Griswold MA, Jakob PM, Heidemann RM, et al. Generalized autocalibrating partially parallel acquisitions (GRAPPA). Magn Reson Med. 2002;47(6):1202-1210.
3 Lustig M, Donoho D, Pauly JM. Sparse MRI: The application of compressed sensing for rapid MR imaging. Magn Reson Med. 2007;58(6):1182-1195.
4 Hammernik K, Klatzer T, Kobler E, et al. Learning a variational network for reconstruction of accelerated MRI data. Magn Reson Med. 2018;79(6):3055-3071.
5 Hammernik, Kerstin, et al. Deep Learning for Parallel MRI Reconstruction. MAGNETOM Flash (75) 4/2019:10–15.
6 Kannengiesser SAR, Mailhe B, Nadar M, et al. Universal iterative denoising of complex-valued volumetric MR image data using supplementary information. Proceedings of the ISMRM, Abstract 1776, 2016.
7 Knoll F, Hammernik K, Zhang C, et al. Deep-learning methods for parallel magnetic resonance imaging reconstruction: A survey of the current approaches, trends, and issues. IEEE Signal Processing Magazine 37.1 (2020): 128–140.

Contact

Nicolas Behl, Ph.D.
Siemens Healthineers
DI MR M&S SYS
Erlangen
Germany
nicolas.behl@siemens-healthineers.com

The DICOM files of the figures in this article are available for download

www.magnetomworld.siemens-healthineers.com > Clinical Corner > Protocols > DICOM Images

Phoenix is a unique *syngo*-tool that allows you to click on an image, drag it into the measurement queue, and instantly duplicate the extracted protocol – TR, TE, bandwidth, number of slices, echo spacing, etc.

- Phoenix ensures reproducibility, e.g., for patient follow-up.
- Phoenix shares optimized protocols on the different MAGNETOM systems you work with.
- Phoenix supports multi-center protocol standardization.

You'll find DICOM images from various systems and all aspects of MRI at magnetomworld.siemens-healthineers.com **> Clinical Corner > Protocols > DICOM Images**

Learn from the experience of other MAGNETOM users

The MAGNETOM World is the community of Siemens Healthineers MR users worldwide, providing you with relevant clinical information. Here you will find application tips and protocols to optimize your daily work. Lectures and presentations from experts in the field will allow you to be exposed to new ideas and alternative clinical approaches.

Put the advantages of the MAGNETOM Wold to work for you!

www.magnetomworld.siemens-healthineers.com

Optimize your clinical protocols by downloading the .exar1 and .edx files shared by leading institutions around the world.
Go to **Clinical Corner > Protocols**

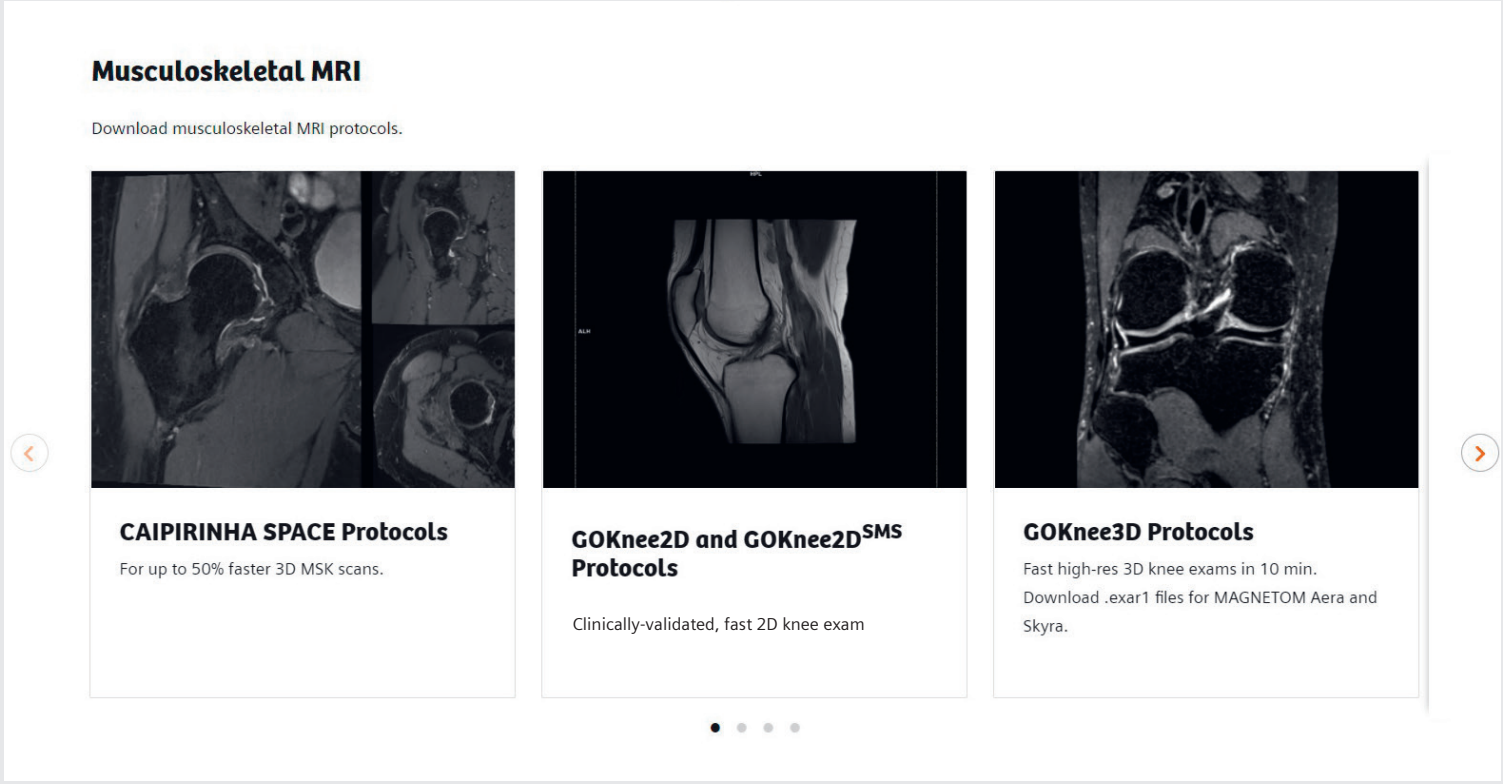

Don’t miss the talks of international experts on all aspects of MSK imaging.
Go to **Clinical Corner > Clinical Talks**

Fast and Efficient MSK Imaging: Tips and Tricks to Squeeze More Performance out of your Scanner

Bac Nguyen;
Oslo University Hospital, Rikshospitalet, Oslo, Norway

Applying State-of-the-Art Acceleration Techniques to Prepare Your MSK MRI Practice for COVID-19 Recovery

Jan Fritz;
NYU Grossmann School of Medicine, New York, NY, USA

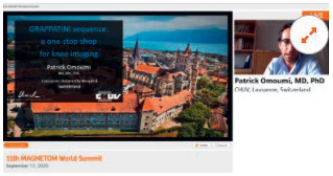

GRAPPATINI Sequence: a One-stop Shop for Knee Imaging

Patrick Omoumi;
CHUV,
Lausanne, Switzerland

The centerpiece of the MAGNETOM World Internet platform consists of MAGNETOM users’ clinical results. Here you will find articles, case reports and clinical methods.
Go to **Clinical Corner > Case Studies**

Thomas Lloyd, et al., (Princess Alexandra Hospital, Brisbane QLD, Australia)

SMS-RESOLVE Tractography for Surgical Management of Brachial Plexus Trauma

Philip Chappel; ZNA Jan Palfijn Hospital, Merksem, Belgium

New Clinical Possibilities and Increased Productivity after Upgrading from MAGNETOM Aera to MAGNETOM Sola Fit

Cristina Mitea, Rik Moonen, et al., Maastricht University Medical Centre, The Netherlands

Imaging of Osteomyelitis with FDG PET-MR

Just a mouse click away you will find application videos and useful tips allowing you to optimize your daily MR examinations.
Go to **Clinical Corner > Application Tips**

Dag Sjølie, Diakonhjemmet Hospital, Radiology Department, Oslo, Norway

How I do It: Imaging Morton’s Neuroma

Corentin Mauris et al. (IRM74 Economic Interest Group, Annecy, France)

Revisiting 3T: Pearls and Pitfalls Compared with 1.5T

Tanja Dütting and Stephan Clasen, (Institute for Diagnostic and Interventional Radiology, Kreiskliniken Reutlingen, Germany)

Experience of Using a New Autopilot Assistance System for Easy Scanning in Brain and Knee MRI Examinations

Compressed Sensing in Metal Hip Imaging: Our Experience

Mustafa M. Almuqbel, RT, (MR), ARRT, Ph.D.[1,2,3]; Tracy R. Melzer, Ph.D.[2,3]; Byron J. Oram, MBChB, FRANZCR[1,4]; Ross J. Keenan, MBChB, FRANZCR[1,2,4]

[1]Pacific Radiology Group, Christchurch, New Zealand
[2]New Zealand Brain Research Institute, Christchurch, New Zealand
[3]Department of Medicine, University of Otago, Christchurch, New Zealand
[4]Department of Radiology, Christchurch Hospital, Christchurch, New Zealand

Introduction

For end stage hip disease, total hip arthroplasty (THA) has become an attractive management option for many patients [1, 2]. While THA offers excellent pain relief and helps a majority of patients to regain some portion of day to day mobility, it is not without complications. About 40% of patients who undergo THA report groin and thigh pain [3, 4]. Despite the development in implant design, fixation approaches, and bearing materials, most prostheses eventually fail [5]. Given this, there is an increasing demand for more accurate diagnosis and visualization prior to hip revision.

Recently, magnetic resonance imaging (MRI) has become the imaging modality of choice for most clinicians to image potential THA-related complications[1] [6, 7]. In one imaging session, MRI can provide useful information about periprosthetic fractures, and osteolysis, postoperative hematoma, disruption of the pseudocapsule, synovitis caused by polyethylene wear and adverse local tissue reactions, periprosthetic masses, bursitis, tendinopathy, and neurovascular compromise [8]. However, MRI near metal comes with a well-known challenge, the susceptibility induced blooming artifact. This artifact hinders image quality and consequently diagnostic accuracy.

Magnetic susceptibility refers to the extent by which a substance is magnetised when exposed to the magnetic field. Different substances exhibit various degrees of magnetic susceptibility when exposed to a static magnetic field [9, 10]. Metallic objects have higher magnetic susceptibility than biological tissues. This induces severe spin dephasing (incoherence) around metallic implants and causes signal drop out and a form of image distortion [11].

In practice, using high bandwidth (BW), thinner slices, smaller field of view, finer matrix and imaging at lower magnetic fields are all helpful protocol adaptions to reduce the metal-induced artifact. However, these changes to the MR sequence lead to reduced signal to noise ratio (SNR) and often increased specific absorption rate (SAR). Therefore, practitioners tend to scan for longer times to mitigate the adverse effects associated with reducing the metal-induced artifact.

syngo WARP is a Siemens Healthineers solution that offers techniques to reduce susceptibility-related distortions. *syngo* WARP comprises

- Turbo Spin Echo (TSE) sequence optimized for imaging in the presence of metal implants
- "View Angle Tilting" or VAT and
- "Slice Encoding for Metal Artifact Correction" or SEMAC[2].

When VAT is added to a turbo spin echo pulse sequence, an additional gradient is applied in the data readout step to correct the in-plane distortion. However, only correcting for the in-plane distortion is not enough. Hence, the SEMAC option has been introduced. SEMAC offers through-plane distortion correction, similar to 3D imaging, where additional phase-encoding steps are added in the third dimension. This provides information on how the slice profile is distorted, which is used later to correct the distortion during the image reconstruction stage. Therefore, the more additional phase-encoding steps, the richer the slice profile, which enhances the distortion correction process. However, while adding additional phase-encoding steps helps in improving the image quality, it requires longer scanning time and additional postprocessing [12, 13].

What is promising is that one can use VAT and SEMAC simultaneously. That is, concurrently correcting

[1]The MRI restrictions (if any) of the metal implant must be considered prior to patient undergoing MRI exam. MR imaging of patients with metallic implants brings specific risks. However, certain implants are approved by the governing regulatory bodies to be MR conditionally safe. For such implants, the previously mentioned warning may not be applicable. Please contact the implant manufacturer for the specific conditional information. The conditions for MR safety are the responsibility of the implant manufacturer, not of Siemens Healthineers.
[2]SEMAC is part of the Advanced WARP package

for in-plane and through-plane metal-induced distortions. However, unlike VAT, SEMAC impacts the scan time dramatically, making the addition of SEMAC to every sequence impractical in clinical settings. However, publications have shown a clear diagnostic benefit of SEMAC protocols for hip and knee joint replacements [14–16]. As a solution to this problem, we present our experience with a "Compressed Sensing" technique for metal hip imaging and its added benefit in improving image quality and reducing scan times.

Although it is beyond the scope of this work to discuss the technical aspects of the Compressed Sensing (CS) technique, briefly CS refers to the ability to reconstruct the image-forming signals with fewer measurements (or samples) than what was classically thought necessary. Therefore, Compressed Sensing is a method to accelerate the MRI procedure by collecting less data (i.e., undersampling *k*-space) while maintaining image quality [17, 18].

[3]Work in progress: the application is currently under development and is not for sale in the U.S. and in other countries. Its future availability cannot be ensured.

Methods

43 patients with total hip arthroplasty (THA) were scanned on a 48-channel 1.5T MAGNETOM Aera system (Siemens Healthcare, Erlangen, Germany). In addition to their clinical imaging protocol (which includes "VAT only" WARP), we acquired additional SEMAC and Compressed Sensing-SEMAC (CS-SEMAC)[3] sequences. The latter being a prototype provided by Siemens Healthineers. All imaging was performed using the 18-channel body coil. Table 1 shows the imaging parameters of these three implemented sequences.

Aim

Combining VAT and SEMAC to achieve both in-plane and through-plane distortion correction is an attractive option; however, adopting such an approach is limited due to the long scan times. Leveraging Compressed Sensing (CS), we aim to explore whether CS-SEMAC[3] can offer improved image quality at reasonable imaging times.

Sequence	VAT only (default protocol)	VAT+SEMAC (12 PES)	VAT+CS-SEMAC (12 PES)	VAT+CS-SEMAC (20 PES)
Imaging plane	Coronal oblique	Coronal oblique	Coronal oblique	Coronal oblique
Image weight	Proton density	Proton density	Proton density	Proton density
Repetition time	2800 ms	2640 ms	3880 ms	3880 ms
Echo time	38 ms	32 ms	32 ms	32 ms
Field of view	240 mm	240 mm	240 mm	240 mm
Slice thickness	3.5 mm	3.5 mm	3.5 mm	3.5 mm
Matrix	320×256	320×256	320×256	320×256
Bandwidth	600 Hz	650 Hz	650 Hz	650 Hz
Flip angle	140	150	135	135
Averages	4	1	1	1
Turbo factor	15	14	21	21
GRAPPA	2	2	Off	Off
Compressed Sensing	Off	Off	On	On
VAT	**50%**	**100%**	**100%**	**100%**
SEMAC additional phase-encoding steps (PES)	**Off**	**12**	**12**	**20**
Echo spacing	7.56 ms	8.06 ms	8.06 ms	8.06 ms
Bandwidth	600 Hz/Px	650 Hz/Px	650 Hz/Px	650 Hz/Px
Scan time (minutes)	**03:20**	**06:50**	**02:50**	**04:25**

Table 1: Imaging parameters
VAT = View Angle Tilting; **SEMAC** = Slice Encoding for Metal Artifact Correction;
PES = Phase-encoding steps; **GRAPPA** = GeneRalized Autocalibrating Partially Parallel Acquisitions

Findings and discussion

VAT-only versus SEMAC:

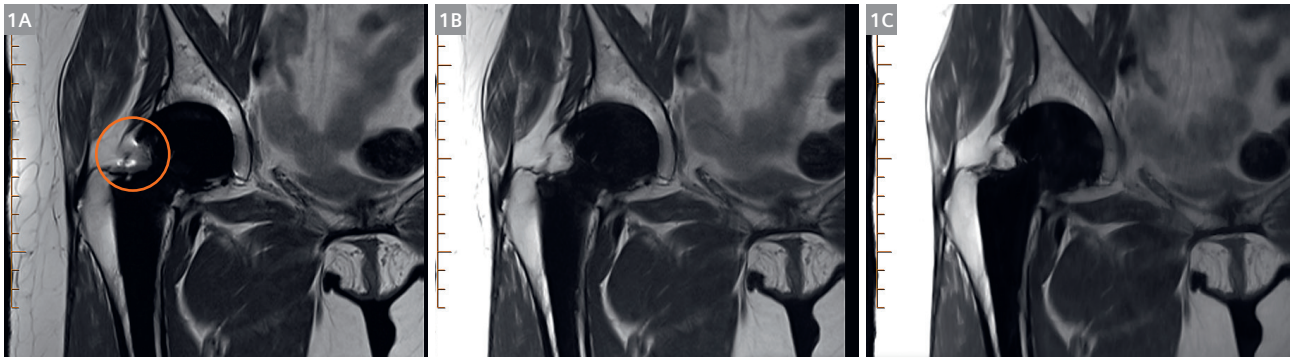

Sequence	Cor PD VAT-only (product)	Cor PD VAT+SEMAC (product)	Cor PD VAT+CS-WARP (WIP)
Quality	Image quality degraded by pile-up artifact (circled in orange).	Artifact reduced.	Artifact markedly reduced.
Time	03:20 min	06:50 min	02:50 min
Overall rating	Still suffers an artifact.	Good artifact reduction, but infeasibly long.	Reduced artifact and short scan time.

1 A 61-year-old female with right total hip arthroplasty (THA). The implant-associated artifact is relatively benign (i.e., relatively subtle susceptibility artifact). However, the VAT-only image (**1A**) shows signal "pile up" caused by the signal aggregation (circled in orange). While the use of the SEMAC sequence (**1B**) was helpful in reducing the "pile up" artifact significantly, the imaging time was unacceptably long in a busy clinical setting. The application of Compressed Sensing (**1C**) resulted in reduced artifact, excellent image quality, and shorter scan time.

SEMAC "with motion" versus CS-SEMAC:

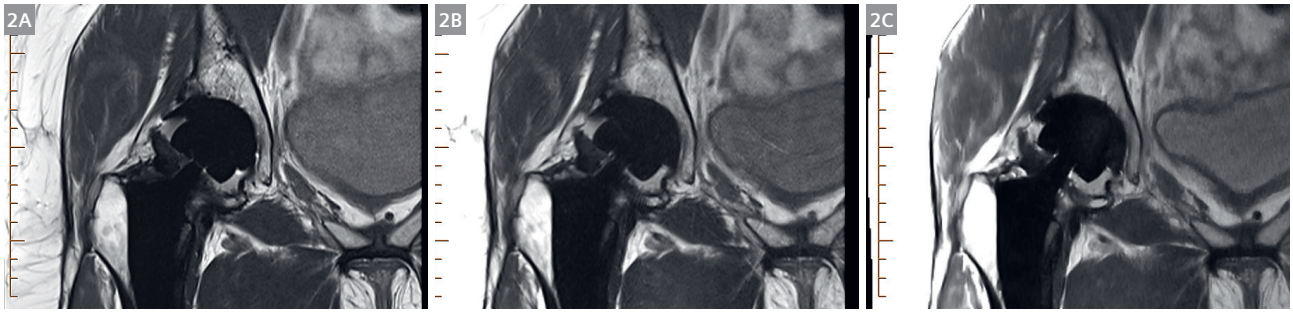

Sequence	Cor PD VAT-only (product)	Cor PD VAT+SEMAC (product)	Cor PD VAT+CS-WARP (WIP)
Quality	Image quality degraded by susceptibility artifact.	Susceptibility artifact with image blurring (due to patient movement).	Mild susceptibility artifact, without patient movement.
Time	03:20 min	06:50 min	02:50 min
Overall rating	Still suffers an artifact.	Patient was in pain and moved during this long scan. We decided not to repeat this scan.	Relative to the VAT-only scan, not only did we achieve better artifact reduction, but we saved 4 minutes by avoiding repeating the long VAT+SEMAC blurry scan.

2 40-year-old female with right total hip arthroplasty (THA). The patient was referred to MRI with right hip pain. The VAT-only image (**2A**) shows a minimal amount of metal-induced artifact in relation to the case in Figure 1. Image (**2B**), took nearly 7 minutes to acquire. Unfortunately the patient moved during this long scan, resulting in motion-degraded images. The Compressed Sensing VAT+SEMAC scan (**2C**) took just 02:50 minutes to collect and was better tolerated by the patient. This case shows the advantage of using Compressed Sensing in accelerating the scan while maintaining and improving image quality. This is especially important in cases where patients are uncomfortable and cannot remain still.

SEMAC versus CS-SEMAC:

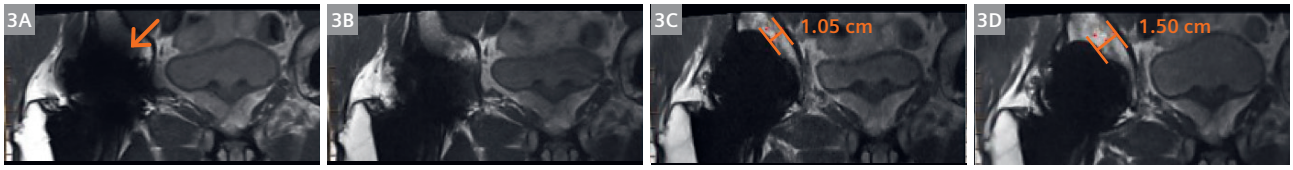

Sequence	Cor PD VAT-only (product)	Cor PD VAT+SEMAC (product)	Cor PD VAT+CS-WARP-12 (WIP)	Cor PD VAT+CS-WARP -20 (WIP)
Quality	Severe susceptibility artifact.	Susceptibility artifact reduced.	Susceptibility artifact reduced, with recovery of pubic bone detail.	Susceptibility artifact reduced, with excellent pubic bone recovery.
Time	03:20 min	06:50 min	02:50 min	04:25 min
Overall rating	Still suffers an artifact.	Despite the artifact reduction, it is still infeasibly long.	Reduced artifact and short scan time.	The gain in near-metal visibility outweighs the 1.75 min extra time added, in our opinion.

3 59-year-old male with right cementless metal-on-metal total hip arthroplasty (THA). The patient enjoyed 8 years of excellent functional outcome after the THA. He was referred to MRI with right groin pain and clunking sensation. The implant-associated artifact is severe. Using the pubic bone as a reference (orange arrow), on the VAT-only image (**3A**), it is difficult to visualize the pubic bone due to the artifact impact on the image. On the VAT+SEMAC image (**3B**), despite the long scan time, only a slight improvement has taken place and the bone detail suffers significant distortion. Implementing CS-SEMAC with 12 phase-encoding steps (**3C**), the bone morphology normalises. Finally, using the CS-SEMAC sequence, we increased phase-encoding steps from 12 to 20 (**3D**); this resulted in a marked improvement in visualisation of the anatomy. When we compared CS-SEMAC-12 to CS-SEMAC-20 images, we achieved 70% morphology recovery (1.05 cm to 1.50 cm). In our opinion, the gain in image quality afforded by the CS-SEMAC-20 sequence outweighs the additional scan time (02:50 min to 04:25 min).

SEMAC versus CS-SEMAC:

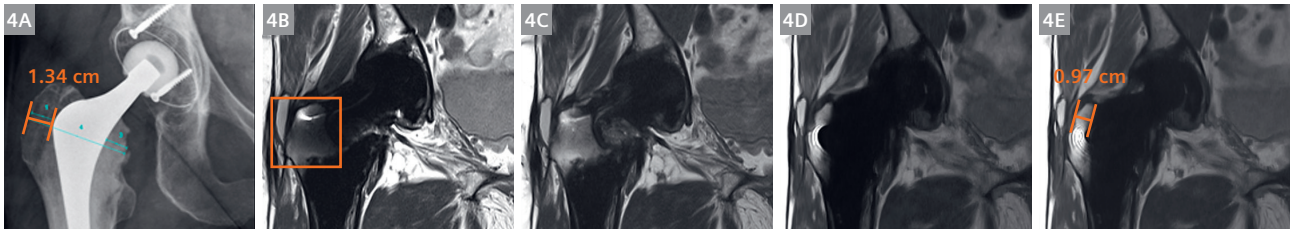

Sequence	Hip Radiograph	Cor PD VAT-only (product)	Cor PD SEMAC (product)	Cor PD VAT+CS-WARP -12 (WIP)	Cor PD VAT+CS-WARP-20 (WIP)
Quality	The greater trochanter measures 1.34 cm.	Severe distortion of the greater trochanter (orange square).	Susceptibility artifact reduced, but the image still suffers an artificial bone distortion similar to the image in 4B.	Greater trochanter image quality improved, it measured 0.86 cm.	Further image quality improvement, with reduced artifact. The greater trochanter measured 0.97 cm.
Time		03:20 min	06:50 min	02:50 min	04:25 min
Overall rating		Still suffers an artifact with misleading greater trochanter measurement – induced by the artifact.	Still suffers an artifact with misleading greater trochanter measurement – induced by the artifact.	The addition of CS-SEMAC allowed for better artifact reduction and more realistic structural measurement around the implant.	Artifact reduction is shown to be directly associated with the number of phase encoding steps in the Compressed Sensing technique.

4 67-year-old female with right total hip arthroplasty (THA). The patient had two dislocations and was referred to MRI to rule out abductor dysfunction. While both the VAT-only and VAT+SEMAC scans (**4B & 4C**) were degraded by geometric distortion and susceptibility artifact, the Compressed Sensing scans (**4D & 4E**) demonstrated a great ability to reduce these artifacts. This resulted in marked improvement in periprosthetic image quality, with mild residual inherent artifact. In the CS-SEMAC scan, despite the increase in the scan time after increasing the number of phase encoding steps from 12 to 20, the gain in the image quality was clinically significant.

Conclusion

Imaging near metals is largely "implant" dependant – some implants induce significantly detrimental artifacts while others result in relatively minor distortion. The recent improvement in imaging techniques such as VAT and SEMAC allowed imaging professionals to correct for both in-plane and through-plane metal-induced artifacts, with a corresponding improvement in diagnostic accuracy. However, acquiring images with VAT and SEMAC combined prolongs the imaging time, which is impractical in many clinical settings.

In this work, we demonstrated the utility of Compressed Sensing (CS) SEMAC technique not only in reducing the scan time, but also in improving image quality. Artifact severity was inversely associated with the number of the phase-encoding steps performed in the Compressed Sensing approach – that is, increasing phase encoding steps reduced artifact severity, but at the expense of increased scan time.

The only challenge we have experienced during our usage of the CS WIP package was the image reconstruction time. While data acquisition is remarkably short, it took a few minutes for the images to reconstruct (on our scanner at least). The reconstruction time is proportional to the number of phase-encoding steps. This has changed completely with the product implementation, where optimized algorithms are exploiting the power of a reconstruction system specifically designed for CS calculations. In conclusion, we are impressed with the image quality and scan times achievable with the CS-SEMAC technique.

Contact

Dr Mustafa Almuqbel
Pacific Radiology Group
151 Leinster road, Strowan
Christchurch, 8014
New Zealand
Tel: +64 3 379 0770
mustafa.almuqbel@pacificradiology.com

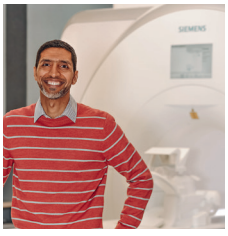

References

1 Mancuso CA, Salvati EA, Johanson NA, Peterson MG, Charlson ME. Patients' expectations and satisfaction with total hip arthroplasty. The Journal of arthroplasty. 1997;12(4):387-96.
2 Krushell R, Bhowmik-Stoker M, Kison C, O'Connor M, Cherian JJ, Mont MA. Characterization of patient expectations and satisfaction after total hip arthroplasty. J Long Term Effects Med Implants. 2016;26(2).
3 Sharkey PF, Hozack WJ, Rothman RH, Shastri S, Jacoby SM. Why are total knee arthroplasties failing today? Clinical Orthopaedics and Related Research®. 2002;404:7-13.
4 Ulrich SD, Seyler TM, Bennett D, Delanois RE, Saleh KJ, Thongtrangan I, et al. Total hip arthroplasties: what are the reasons for revision? International orthopaedics. 2008;32(5):597-604.
5 Brown TE, Larson B, Shen F, Moskal JT. Thigh pain after cementless total hip arthroplasty: evaluation and management. JAAOS-Journal of the American Academy of Orthopaedic Surgeons. 2002;10(6):385-92.
6 Siegel MJ. Magnetic resonance imaging of musculoskeletal soft tissue masses. Radiologic Clinics Of North America. 2001;39(4):701-20.
7 Bitar R, Leung G, Perng R, Tadros S, Moody AR, Sarrazin J, et al. MR pulse sequences: what every radiologist wants to know but is afraid to ask. Radiographics. 2006;26(2):513-37.
8 Fritz J, Lurie B, Miller TT, Potter HG. MR imaging of hip arthroplasty implants. Radiographics. 2014;34(4):E106-E32.
9 Le Bihan D, Poupon C, Amadon A, Lethimonnier F. Artifacts and pitfalls in diffusion MRI. Journal of Magnetic Resonance Imaging: An Official Journal of the International Society for Magnetic Resonance in Medicine. 2006;24(3):478-88.
10 Dietrich O, Reiser MF, Schoenberg SO. Artifacts in 3-T MRI: physical background and reduction strategies. European journal of radiology. 2008;65(1):29-35.
11 Smith MR, Artz NS, Wiens C, Hernando D, Reeder SB. Characterizing the limits of MRI near metallic prostheses. Magn Reson Med. 2015;74(6):1564-73.
12 Bachschmidt T, Lipps F, Nittka M. *syngo* WARP: Metal Artifact Reduction Techniques in Magnetic Resonance Imaging. Magnetom Flash. 2012;2:24-5.
13 Jungmann PM, Ganter C, Schaeffeler CJ, Bauer JS, Baum T, Meier R, et al. View-angle tilting and slice-encoding metal artifact correction for artifact reduction in MRI: experimental sequence optimization for orthopaedic tumor endoprostheses and clinical application. PloS one. 2015;10(4):e0124922.
14 Sutter R, Ulbrich EJ, Jellus V, Nittka M, Pfirrmann C: Reduction of metal artifacts in patients with total hip arthroplasty with slice-encoding metal artifact correction and view-angle tilting MR imaging. Radiology. 2012;265(1).
15 Gupta A, Subhas N, Primak AN, Nittka M, Liu K. Metal artifact reduction standard and advanced magnetic resonance and computed tomography techniques. Radiol Clin N Am 53 (2015) 531–547.
16 Fritz J, Fritz B, Thawait GK, Rathel E, Gilson WD, Nittka M, Mont MA. Advanced metal artifact reduction MRI of metal-on-metal hip resurfacing arthroplasty implants: compressed sensing acceleration enables the time-neutral use of SEMAC. Skeletal Radiol. 2016;45(10):1345-56.
17 Lustig M, Donoho D, Pauly JM. Sparse MRI: The application of compressed sensing for rapid MR imaging. Magnetic Resonance in Medicine: An Official Journal of the International Society for Magnetic Resonance in Medicine. 2007;58(6):1182-95.
18 Jaspan ON, Fleysher R, Lipton ML. Compressed sensing MRI: a review of the clinical literature. The British journal of radiology. 2015;88(1056):20150487.

Learn more about Musculoskeletal MR Imaging

Lectures and presentations given at the MAGNETOM World Summit are available on-demand

Fast and Efficient MSK Imaging: Tips and Tricks to Squeeze More Performance out of Your Scanner
Bac Nguyen (Oslo University Hospital, Rikshospitalet, Oslo, Norway)

Sports Imaging – the Whole Picture
Charles Ho (Steadman Philippon Research Inst., Vail, CO, USA)

MSK Related Rheumatoid Arthritis and Related Cardiac Problems
Patrick Veit-Haibach (University of Toronto, Canada)

GRAPPATINI Sequence: a One-Stop Shop for Knee Imaging
Patrick Omoumi (Lausanne University Hospital, Lausanne, Switzerland)

Applying State-of-the-Art Acceleration Techniques to Prepare Your MSK MRI Practice for COVID-19 Recovery
Jan Fritz (New York University, New York, NY, USA)

Don't miss this valuable source of information
www.siemens-healthineers.com/MWS2020-recordings

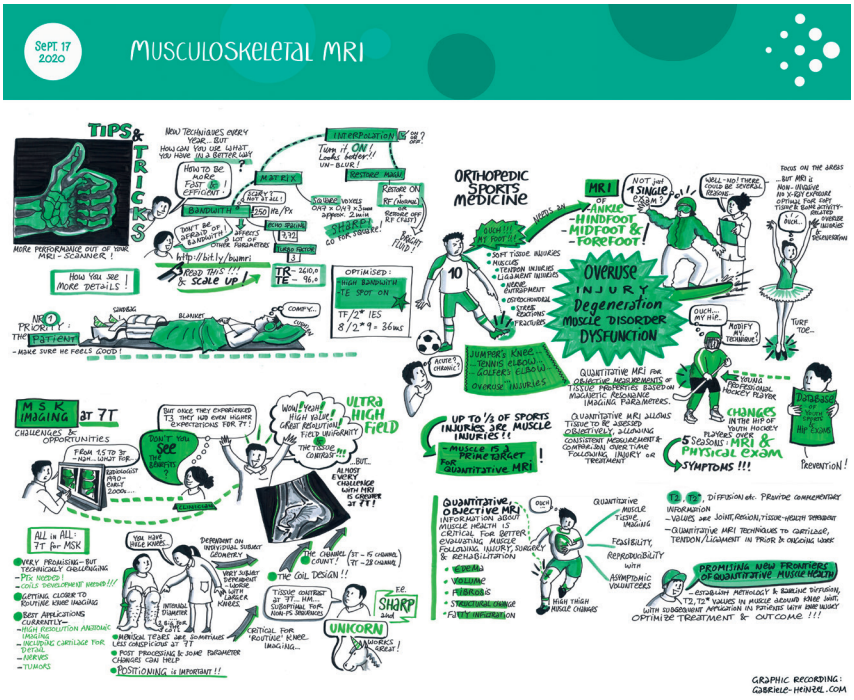

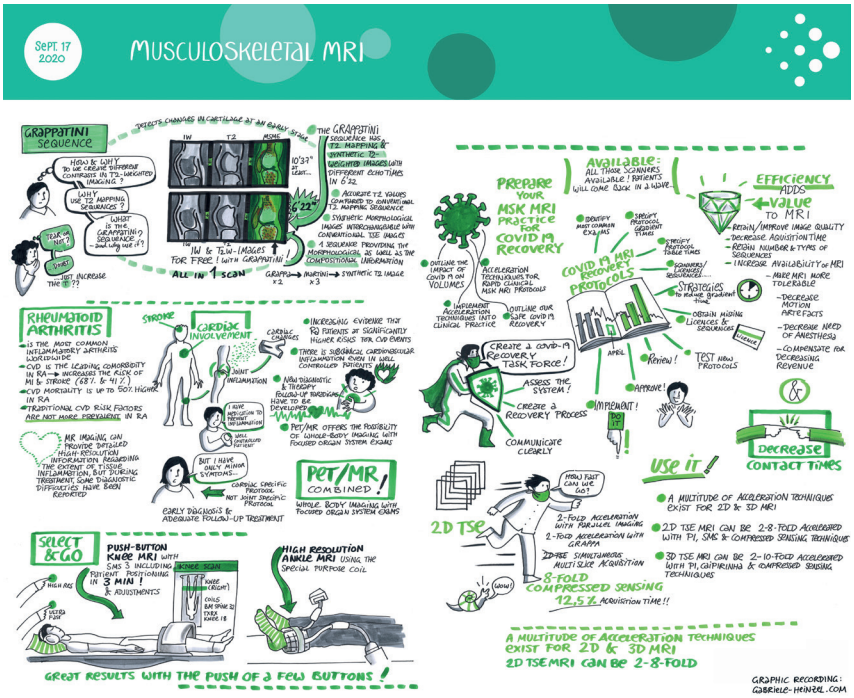

Graphic recording:
www.gabriele-heinzel.com

Not for distribution in the US

On account of certain regional limitations of sales rights and service availability, we cannot guarantee that all products included in this brochure are available through the Siemens sales organization worldwide. Availability and packaging may vary by country and is subject to change without prior notice. Some/All of the features and products described herein may not be available in the United States.

The information in this document contains general technical descriptions of specifications and options as well as standard and optional features which do not always have to be present in individual cases, and which may not be commercially available in all countries.

Due to regulatory reasons their future availability cannot be guaranteed. Please contact your local Siemens organization for further details.

Siemens reserves the right to modify the design, packaging, specifications, and options described herein without prior notice. Please contact your local Siemens sales representative for the most current information.

Note: Any technical data contained in this document may vary within defined tolerances. Original images always lose a certain amount of detail when reproduced.

Siemens Healthineers Headquarters
Siemens Healthcare GmbH
Henkestr. 127
91052 Erlangen, Germany
Phone: +49 9131 84-0
siemens-healthineers.com

Published by Siemens Healthcare GmbH · Order No. A91MR-000047-100C-1-7600 · Printed in Germany · 10942 0721 ·

siemens.com/magnetom-world